

Long-Range Ferromagnetism of Mn_{12} Acetate Single-Molecule Magnets under a Transverse Magnetic Field

F. Luis,^{1,*} J. Campo,¹ J. Gómez,² G. J. McIntyre,³ J. Luzón,¹ and D. Ruiz-Molina²

¹*Instituto de Ciencia de Materiales de Aragón, CSIC-Universidad de Zaragoza, 50009 Zaragoza, Spain*

²*Institut de Ciència de Materials de Barcelona, Campus de la UAB, Bellaterra 08193, Spain*

³*Institut Laue Langevin, 6 rue Jules Horowitz, 38042 Grenoble, France*

(Received 10 February 2005; revised manuscript received 23 May 2005; published 21 November 2005)

We use neutron diffraction to probe the magnetization components of a crystal of Mn_{12} single-molecule magnets. Each of these molecules behaves, at low temperatures, as a nanomagnet with spin $S = 10$ and strong anisotropy along the crystallographic c axis. The application of a magnetic field H_{\perp} perpendicular to c induces quantum tunneling between opposite spin orientations, enabling the spins to attain thermal equilibrium. For $T \approx 0.9(1)$ K, this equilibrium state shows spontaneous magnetization, indicating the onset of ferromagnetism. These long-range magnetic correlations nearly disappear for $\mu_0 H_{\perp} \geq 5.5$ T, possibly suggesting the existence of a quantum critical point.

DOI: [10.1103/PhysRevLett.95.227202](https://doi.org/10.1103/PhysRevLett.95.227202)

PACS numbers: 75.45.+j, 75.30.Kz, 75.50.Xx

Magnetic nanostructured materials have opened new frontiers for science and technology, due to their unique size-dependent properties and the emergence of quantum phenomena [1]. Several fundamental problems, however, remain to be understood. Of particular interest is the observation of phase transitions induced by interactions between nanoscopic magnets in dense arrays. A crucial question here is the mechanism by which the ordered equilibrium phase is attained. For very small magnetic clusters, zero-point quantum fluctuations (e.g., quantum tunneling) are expected to dominate the relaxation process at very low temperatures [2]. Eventually, these fluctuations might even suppress long-range order provided they become sufficiently strong against both interparticle interactions and decoherence [3]. Such a quantum critical point has been observed for model Ising ferromagnets [4], but its existence remains uncertain for arrays of nanomagnets. Understanding the interplay between ordering and quantum fluctuations can be important for applications of these nanomagnets in ultrahigh-density magnetic recording and quantum computation, when it is necessary to control the quantum behavior of entangled interacting qubits.

Usually, however, these phenomena are masked by the particle's size distribution and disorder present in even the most homogeneous samples [5]. By contrast, molecular magnetic clusters [6,7] are ideal candidates for these studies [8,9]. The cluster of Mn_{12} acetate [10], the first and most extensively studied member of the family of single-molecule magnets, contains 12 manganese atoms linked via oxygen atoms, with a sharply defined and *monodisperse* size. At low temperatures, each of them exhibits the typical behavior of a magnetic nanoparticle, such as slow magnetic relaxation and hysteresis, due to the combination of an $S = 10$ magnetic ground state with appreciable magnetic anisotropy. And finally, they organize to form tetragonal molecular *crystals*. Since molecular spins couple via dipolar interactions, these crystals are nearly perfect real-

izations, with magnetic units of mesoscopic size, of the Ising quantum model.

Long-range magnetic order, however, has not been observed for Mn_{12} yet. One reason is that the spin reversal via resonant quantum tunneling [11–14] becomes extremely slow at low temperatures (of order 2 months at $T = 2$ K). For the time scales $\tau_c \sim 10^2$ – 10^4 s of a typical experiment, the spins are unable to attain thermal equilibrium below a blocking temperature $T_B \sim 3$ K, higher than the ordering temperature T_c . It has also been argued [9] that hyperfine bias caused by randomly frozen Mn nuclear spins might hinder the occurrence of long-range order in Mn_{12} . Here we circumvent these experimental problems by the application of a transverse magnetic field H_{\perp} that promotes quantum tunneling of the molecular spins. We report neutron diffraction data that point to the existence of long-range ferromagnetic order below $T_c \approx 0.9(1)$ K and $\mu_0 H_c \sim 5.5(5)$ T.

Magnetic diffraction of thermal neutrons is a suitable tool for these studies because it can probe the magnetization along the anisotropy axis [15] and accurately determine the crystal's orientation. The $\sim 0.5 \times 0.5 \times 1.5$ mm³ single crystal of deuterated Mn_{12} acetate, $[\text{Mn}_{12}(\text{CD}_3\text{COO})_{16}(\text{D}_2\text{O})_4\text{O}_{12}] \cdot 2\text{CD}_3\text{COOD} \cdot 4\text{D}_2\text{O}$, was prepared following the original method of Lis [10]. It was glued to a copper rod in good thermal contact with the mixing chamber of a ³He-⁴He dilution refrigerator, giving access to the temperature range $45 \text{ mK} \leq T \leq 4$ K. The c axis was carefully oriented to be perpendicular to the vertical field $0 \leq \mu_0 H_{\perp} \leq 6$ T applied by a superconducting magnet. From the orientation matrix measured at zero field and $T = 4$ K, we estimate that the crystallographic ($\bar{1}10$) direction lay within $0.1(1)^\circ$ of the magnet axis. Stray magnetic fields arising from Earth's magnetic field or other sources were of order 0.5 G.

At any temperature $T \leq 4$ K, we measured a series of Bragg diffraction reflections as a function of H_{\perp} [16]. Each

reflection (hkl) contains nuclear I_N and magnetic I_m contributions. The former contains information about atomic order, whereas the latter is proportional to the square of the magnetization components perpendicular to the (hkl) direction. The nuclear contribution can be obtained by measuring the intensity at zero field in the paramagnetic phase (see Fig. 1). By subtracting this, I_m can be estimated at any field and temperature.

Given the strong anisotropy of Mn_{12} , the magnetization must be confined in the plane defined by the anisotropy axis c and the magnetic field, with components M_z and M_\perp , respectively. The experimental protocol followed for every reflection line is illustrated in Fig. 1, where we plot raw rocking curves for the $(\bar{2}\bar{2}0)$ reflection. For this reflection, the momentum transfer is orthogonal to that plane. In addition, it has a very small nuclear contribution. Therefore, I_m must be sensitive to both M_z and M_\perp . At 4 K, $I_m \propto (\mu_0 H_\perp)^2$, as expected, since $M_z = 0$ in the paramagnetic state and M_\perp is proportional to H_\perp . At 100 mK, by contrast, a large additional contribution to I_m shows up for $\mu_0 H_\perp < 5$ T. Since M_\perp is nearly independent of T (see the inset of Fig. 2), the additional magnetic diffracted intensity reflects the onset of a nonzero M_z . Furthermore, this low- T contribution shows hysteresis. Indeed, as shown in Fig. 1, I_m data measured while in-

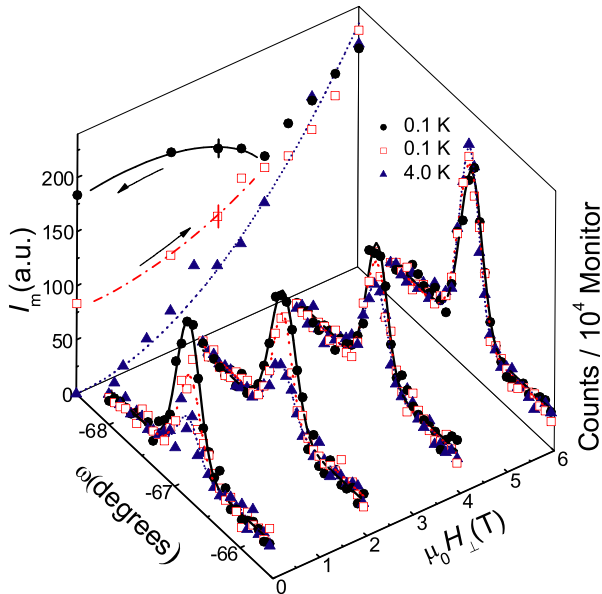


FIG. 1 (color online). Rocking curves for the $(\bar{2}\bar{2}0)$ reflection measured at two different temperatures and four magnetic fields. The counting statistics are typical for such a small crystal under these conditions. The lines are Gaussian fits. Numerical integration of these rocking curves gives the diffracted intensity I . The magnetic diffraction intensities I_m were obtained at each temperature and field by subtracting from the total intensity the value measured at 4 K and $\mu_0 H_\perp = 0$. \blacktriangle , $T = 4$ K; \square and \bullet , $T = 100$ mK measured while increasing and then decreasing H_\perp , respectively. The dotted line is a least-squares fit to a parabola $A(\mu_0 H_\perp)^2$.

creasing H_\perp after the sample was cooled at zero field from $T \approx 1$ K, lie clearly below those measured while decreasing it, merging approximately at $\mu_0 H_\perp = 4(1)$ T. The hysteresis means that spins can attain equilibrium within the experimental time $\tau_e \approx 7 \times 10^3$ s only above $\mu_0 H_\perp = 4$ T. The fact that this field-induced “jump to equilibrium” occurs at approximately the same field for $T = 100$ mK and $T = 600$ mK confirms that relaxation proceeds via temperature-independent tunneling processes [17,18].

To obtain M_z and M_\perp as a function of magnetic field (Fig. 2) and temperature (Fig. 3), several reflection lines were simultaneously fitted and the results calibrated against SQUID magnetization measurements performed at 4 K. At our minimum temperature $T = 47$ mK, M_z is approximately zero for $\mu_0 H_\perp \geq 5.5(5)$ T, and then it increases when decreasing $\mu_0 H_\perp$, reaching $16\mu_B$ per molecule at zero field. The temperature dependence of this zero field M_z is shown in Fig. 3. It is approximately constant until it begins decreasing sharply for $T \geq 0.6$ K. Above 1 K, as at 4 K, the fit gives $M_z \sim 0$.

These experiments show the existence of a net magnetization along the anisotropy axis. The qualitative resemblance between M_z vs $\mu_0 H_\perp$ and M_z vs T curves is typical of quantum ferromagnetic systems [4]. However, for such a strong anisotropy, any deviation of the crystal from the perpendicular orientation can induce, at $\mu_0 H_\perp > 4$ T, some magnetic polarization along the anisotropy axis [18,19] that would then freeze below 4 T. We know this deviation from “high”-temperature diffraction data to be

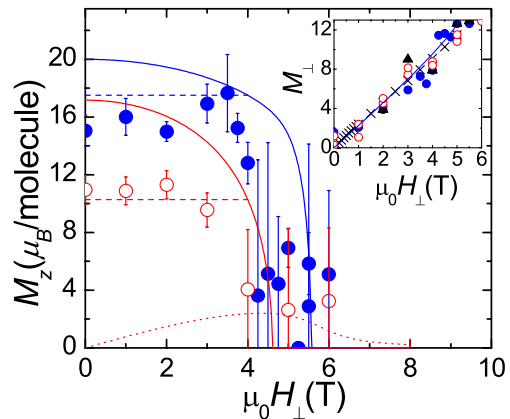


FIG. 2 (color online). Longitudinal magnetization M_z of Mn_{12} acetate measured while decreasing the transverse magnetic field from 6 T. \bullet and \circ are for $T = 47$ and 600 mK, respectively. Solid lines are calculated using Eq. (1) and the parameters given in the text. Horizontal dashed lines show M_z calculated at 4 K, below which spins are “frozen” by the anisotropy energy barriers. The dotted line shows M_z induced at $T = 600$ mK by the misalignment of the crystal (0.1°) in the case of no interactions [$J_{\text{eff}} = 0$ in Eq. (1)]. Inset: \times , perpendicular magnetization M_\perp obtained at $T = 4$ K with a SQUID magnetometer. Data obtained from neutron diffraction are also shown: \bullet , $T = 47$ mK; \circ , $T = 600$ mK; \blacktriangle , $T = 4$ K.

smaller than 0.1° in our sample. In Figs. 2 and 3 we show that such misalignment alone would give rise to a much smaller M_z than what we measure at $T > 100$ mK. Actually, there is no misalignment that could consistently account for all experimental data. Indeed, to account for M_z measured at, say, 0.35 K and 4 T, a deviation of at least 0.5° from perfect orientation is required. However, M_z would then decrease slowly with increasing T and remain $\geq 7\mu_B$ up to 1 K, in sharp contrast with the abrupt decrease observed experimentally (Fig. 3). The small M_z measured for $\mu_0 H_\perp = 4$ T above 500 mK gives an upper misalignment bound of about 0.2° , in agreement with neutron diffraction. Also the difference between the M_z vs T curves obtained at $\mu_0 H_\perp = 4$ T and zero field would not be easy to explain if the ground state were paramagnetic. The increase of M_z with decreasing field shows that spins tend to polarize as they approach equilibrium at zero field. The existence of long-range magnetic order is also supported by the finite temperature intercept [0.8(1) K] of the reciprocal parallel susceptibility shown in Fig. 3(b). Our data therefore strongly suggest that Mn_{12} acetate becomes a ferromagnet for sufficiently low temperatures and magnetic fields. The ferromagnetic nature of the ordered phase agrees with theoretical predictions [8], which, however, predict $T_c \sim 0.45$ K, lower than observed. The discrepancy might arise from the fact that Mn_{12} molecules are extended nanoscopic objects and not pointlike spins [20]. It is worth mentioning that the relatively strong hyperfine interactions do not prevent the ordering of Mn_{12} molecular spins probably because, as has been observed recently [2,17], Mn nuclear spins also relax rapidly to equilibrium when tunneling rates are sufficiently fast.

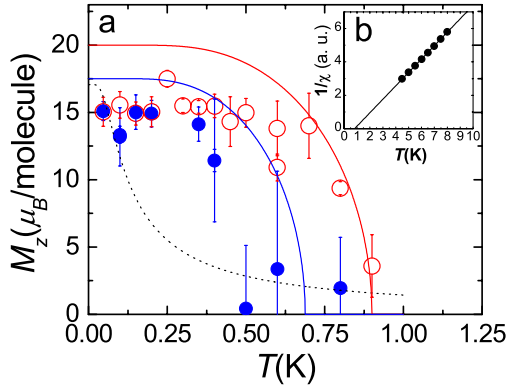


FIG. 3 (color online). (a) Longitudinal magnetization M_z obtained from neutron diffraction data measured at $\mu_0 H_\perp = 0$ (○) and 4 T (●). Measurements were recorded after cooling the sample in zero field and subsequently applying $\mu_0 H_\perp = 6$ T before setting the final field. The dotted line shows M_z arising from the misalignment (0.1°) of the crystal at $\mu_0 H_\perp = 4$ T. Solid lines are calculations (for perfect orientation) that include interactions via the mean-field Hamiltonian (1). (b) Reciprocal parallel susceptibility measured at $T > 4.5$ K (i.e., for equilibrium conditions) along the c axis. The line is a least-squares linear fit, giving $T_c = 0.8(1)$ K.

This qualitative interpretation can be put on a solid basis with the help of theoretical calculations. A simple way to introduce interactions in the analysis is by making use of a mean-field approximation,

$$\mathcal{H} = -DS_z^2 + C(S_+^4 + S_-^4) - g\mu_0\mu_B(H_x S_x + H_y S_y) - J_{\text{eff}}\langle S_z \rangle S_z, \quad (1)$$

where D and C are the uniaxial and in-plane anisotropy constants, $g = 2$ is the gyromagnetic ratio, H_x and $H_y \approx H_\perp/\sqrt{2}$ are the magnetic field components along a and b , J_{eff} is a mean-field interaction parameter, and $\langle S_z \rangle = M_z/g\mu_B$ is the thermal statistical average of S_z . We estimated $D = 0.62k_B$ by fitting the perpendicular magnetization measured at 4 K, while C has been set to 2.5×10^{-4} K in order to fit the critical field $\mu_0 H_c = 5.5$ T. These are of the same order as the values obtained by spectroscopic techniques [21]. We also set $J_{\text{eff}} \approx 4.5 \times 10^{-3}k_B$ which gives $T_c \sim 0.9$ K. We notice that a reasonably good fit of the temperature dependent M_z would be achieved by setting T_c between 0.75 and 0.9 K.

We have calculated M_z and M_\perp by performing a numerical diagonalization of Eq. (1) followed by a self-consistent calculation of the statistically averaged spin components. Field- and temperature-dependent calculations account reasonably well for M_z and M_\perp , predicting, in particular, the vanishing of M_z at either H_c or T_c . The incomplete saturation of M_z at zero field arises probably from “down” spins that remain frozen below $\mu_0 H_\perp = 4$ T because the quantum tunneling rates become too slow at such low fields. We face here the curious situation that quantum fluctuations, which can eventually suppress magnetic order, are nevertheless necessary to attain equilib-

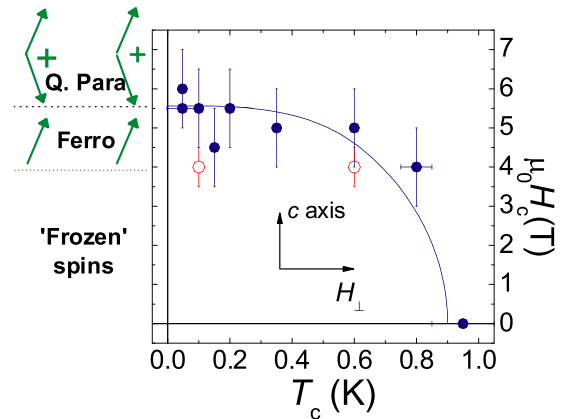


FIG. 4 (color online). Magnetic phase diagram of Mn_{12} acetate. The solid dots show the critical magnetic field $\mu_0 H_c$ at which the longitudinal magnetization is observed to vanish at each temperature. The open dots give the irreversibility field, below which spins are not in equilibrium. The solid line was obtained from magnetization curves calculated with a mean-field model [Eq. (1)].

rium. In Fig. 4, we show the magnetic phase diagram of Mn_{12} acetate obtained from our experiments. The application of a perpendicular field tends to shift T_c significantly towards lower temperatures. As before, the mean-field calculations reproduce reasonably well the overall features.

Summing up, our experiments on Mn_{12} nanomagnets show the existence of a ferromagnetic phase below $\sim 0.75\text{--}0.9$ K that can be suppressed by the application of an external magnetic field. Deciding if this field-induced transition is driven purely by quantum fluctuations requires measuring the critical behavior of M_z [3], which is clearly beyond the sensitivity of the present experiment. What we do observe is that, above $\mu_0 H_c \sim 5.5$ T, the order parameter M_z vanishes even at the lowest accessible temperatures ($T > 47$ mK in our case). We note that $\mu_0 H_c$ is about two thirds of the anisotropy field $2SD/g\mu_B \sim 9$ T that would be required to saturate the Mn_{12} spins along a hard axis if they were *classical* spins. In fact, as shown in the inset of Fig. 2, M_{\perp} is still far from saturation at H_c . These facts and the agreement with mean-field calculations make it plausible that quantum fluctuations can suppress long-range order. Within this interpretation, M_z vanishes because the magnetic ground state becomes a superposition of “spin-up” and “spin-down” states. Previously, the existence of quantum superpositions of spin states was derived from the detection of the ensuing tunnel splitting Δ [17,22,23], while here we have monitored the vanishing of the z spin component.

Arrays of larger nanomagnets, such as magnetic nanoparticles, should show similar collective magnetic phenomena [24], provided they are sufficiently ordered and monodisperse, requirements that appear to be within the reach of modern synthetic procedures [5]. However, besides indications of the collective, spin-glass-like nature of the magnetic relaxation [25], no clear-cut experimental evidence for long-range order has been found yet. The present and some other recent results [2] show that bottom-up synthesis can provide physical realizations of these “superferromagnets,” albeit on a smaller size scale. Furthermore, quantum dynamics can be used to overcome the slow relaxation and to switch between the ordered and paramagnetic phases.

The authors are grateful to J.L. Ragazzoni and D. Culebras for technical assistance. We acknowledge useful comments on this work by J.F. Fernández. This work is part of the research Project No. MAT02-433 funded by Spanish MCyT. It was partly supported by the European Commission under Project No. IST-NANOMAGIQC. Financial support of the ILL for the preparation of the samples is acknowledged.

*Corresponding author.

Electronic address: fluis@unizar.es

- [1] E.M. Chudnovsky and J. Tejada, *Macroscopic Quantum Tunneling of the Magnetic Moment* (Cambridge University Press, Cambridge, 1998).
- [2] M. Evangelisti *et al.*, Phys. Rev. Lett. **93**, 117202 (2004).
- [3] S.L. Sondhi, S.M. Girvin, J.P. Carini, and D. Sahar, Rev. Mod. Phys. **69**, 315 (1997).
- [4] D. Bitko, T.F. Rosenbaum, and G. Aeppli, Phys. Rev. Lett. **77**, 940 (1996).
- [5] S. Sun, C.B. Murray, D. Weller, L. Folks, and A. Moser, Science **287**, 1989 (2000).
- [6] G. Christou, D. Gatteschi, D.N. Hendrickson, and R. Sessoli, MRS Bull. **25**, 66 (2000).
- [7] D. Gatteschi and R. Sessoli, Angew. Chem., Int. Ed. **42**, 268 (2003).
- [8] J.F. Fernández and J.J. Alonso, Phys. Rev. B **62**, 53 (2000).
- [9] X. Martínez-Hidalgo, E.M. Chudnovsky, and A. Aharony, Europhys. Lett. **55**, 273 (2001).
- [10] T. Lis, Acta Crystallogr. Sect. B **36**, 2042 (1980).
- [11] J.R. Friedman, M.P. Sarachik, J. Tejada, and R. Ziolo, Phys. Rev. Lett. **76**, 3830 (1996).
- [12] J.M. Hernández *et al.*, Europhys. Lett. **35**, 301 (1996).
- [13] L. Thomas *et al.*, Nature (London) **383**, 145 (1996).
- [14] L. Thomas, A. Caneschi, and B. Barbara, Phys. Rev. Lett. **83**, 2398 (1999).
- [15] R.A. Robinson, P.J. Brown, D.N. Argyriou, D.N. Hendrickson, and S.M.J. Aubin, J. Phys. Condens. Matter **12**, 2805 (2000).
- [16] Neutron diffraction experiments were carried out on the diffractometer D10 at the Institut Laue Langevin. We worked in a two-axis normal-beam configuration at a neutron wavelength of 2.36 Å.
- [17] F. Luis, F.L. Mettes, J. Tejada, D. Gatteschi, and L.J. de Jongh, Phys. Rev. Lett. **85**, 4377 (2000).
- [18] I. Chiorescu, R. Giraud, A. Jansen, A. Caneschi, and B. Barbara, Phys. Rev. Lett. **85**, 4807 (2000).
- [19] W. Wernsdorfer, N.E. Chakov, and G. Christou, Phys. Rev. B **70**, 132413 (2004).
- [20] Approximating Mn_{12} by pointlike spins gives interaction energies within 2% of the exact result only when the intermolecular distances exceed 5 lattice parameters. For shorter distances, the disklike shape of the Mn_{12} molecule reinforces dipolar interactions along the a or b axes with respect to interactions along c .
- [21] A.L. Barra, D. Gatteschi, and R. Sessoli, Phys. Rev. B **56**, 8192 (1997).
- [22] E. Del Barco *et al.*, Europhys. Lett. **47**, 722 (1999).
- [23] G. Bellessa, N. Vernier, B. Barbara, and D. Gatteschi, Phys. Rev. Lett. **83**, 416 (1999).
- [24] S. Mørup, Hyperfine Interact. **90**, 171 (1994).
- [25] T. Jonsson *et al.*, Phys. Rev. Lett. **75**, 4138 (1995).